World Journal of Engineering and Technology, 2023, 11, 989-999
https://www.scirp.org/journal/wjet
ISSN Online: 2331-4249
ISSN Print: 2331-4222

Research on the Aerodynamic Characteristics of Leading Edge and Bulge of Ram-Air Parafoil Based on CFD

Lei Ding, Lingrui Chen, Yalei Bai, Huimin Yao, Chuanyu Gao

College of Aerospace Engineering, Nanjing University of Aeronautics and Astronautics, Nanjing, China
Email: dinglei99@nuaa.edu.cn

How to cite this paper: Ding, L., Chen, L.R., Bai, Y.L., Yao, H.M. and Gao, C.Y. (2023) Research on the Aerodynamic Characteristics of Leading Edge and Bulge of Ram-Air Parafoil Based on CFD. *World Journal of Engineering and Technology*, **11**, 989-999.
https://doi.org/10.4236/wjet.2023.114065

Received: October 6, 2023
Accepted: November 27, 2023
Published: November 30, 2023

Abstract

This study focuses on the aerodynamic characteristics and flow mechanism of three different configurations of ram-air parafoil with open/closed air inlet and bulges. Firstly, we designed a special parafoil configuration for this study. Then we used numerical simulation to obtain the aerodynamic data of three parafoils at different angles of attack, and studied the influence of the bulge and the leading edge open/closed inlet on the aerodynamic performance of the ram-air parafoil. Finally, we study the flow mechanism of the ram-air parafoil through the pressure distribution and flow field. The results of the study show that compared with the aerodynamic parameters of the parafoil without bulges, the optimal angle of attack of the two parafoils with bulges is increased by 4˚, the maximum lift to drag ratio of the parafoil with closed leading edge is reduced by about 4.3% and the optimal angle of attack is reduced by about 2˚. The maximum lift to drag ratio of the parafoil with open leading edge is reduced by about 23.6% and the stalling angle of attack is reduced by about 4˚. The pressure on the surface of a ram-air parafoil with open leading edge inlet is the highest.

Keywords

Ram-Air Parafoil, Numerical Simulation, Aerodynamic Characteristics, Flow Mechanism

1. Introduction

Ram-air parafoil is different from the traditional parachute with large open canopy, its canopy is mainly connected with a number of rib widths through the upper and lower airfoils to form a number of air chambers, with the leading edge open and the trailing end closed, relying on the open leading edge of the notch air intake to form a stamping air in flight, and in the air chamber, due to the low permeability of the parafoil surface material, the formation of a hysteresis pressure to maintain the shape of canopy. When filled with air, a ram-air parafoil is similar to a curved wing, and can generate enough lift. At the same time, because the material of the ram-air parafoil is mostly lightweight fabric, it does not have excessive mass itself, which makes the ram-air parafoil have efficient gliding performance. Compared with the traditional parachute, the ram-air parafoil has controllability and high gliding ability. With the rapid development of aerospace technology and the continuous expansion of related technology application fields, the rammed parafoil has a wide range of applications in precision airdrop, spacecraft recovery and civil fields.

C Matos [1] used the method of inverted hanging parafoil for wind tunnel measurement, used a three-dimensional stereo ranging video imaging technology to determine the angle of attack of the parafoil during the test, and changed the angle of attack of the parafoil by pulling the control rope backwards. This study measured the lift-to-drag ratio data of the parafoil, captured the collapse process of the parafoil's leading edge at a low angle of attack, and measured the stalling angle of attack. This inverted measurement method can effectively expand the parafoil to an ideal state. The research results are applicable to validation of CFD numerical methods. J Seidel [2] studied the wind tunnel test of a leading-edge open wing section with a parafoil reference profile, measured its aerodynamic forces and moments at different angles of attack, established base data for a parafoil wing profile, and evaluated the effectiveness by use air bleed vents as a parafoil control mechanism. K Bergeron [3] conducted a study on the rigid closed parafoil wing section, designed a wind tunnel test with or without a leading edge cut and whether the trailing edge was downward, and filled the aerodynamic database to provide data for numerical simulation verification. To summarize, the early research methods for the performance evaluation of ram-air parafoil include wind tunnel test, air drop test, etc. [4] [5]. The test methods are closer to the real situation, but the cost is expensive and the development cycle is long [6] [7]. There is a lack of test data and fewer test methods in China about the parafoil test. Therefore, we established a new parafoil configuration, and carried out CFD numerical simulation to study the aerodynamic characteristics and flow mechanism of the designed parafoil. It provides the theoretical data support for the simulation calculation method and design of the parafoil.

2. Model Design of the Research Object

Object 1: In this paper, the ideal non bulge unfolding state of the parafoil is designed. The design parameters of the canopy system are shown in **Table 1**, and the computational model is shown in **Figure 1**.

Object 2: This paper designs the unfolding and bulging state of the parafoil. Due to the influence of the flexibility factor, the canopy of the parafoil expands

Table 1. Parameters of canopy.

Inverted dihedral	Canopy area	Leading edge sweep Angle	Trailing edge forward sweep Angle	Aspect ratio	Mean chord
$\beta = 22^{\circ}$	$S = 30.8\ m^2$	$\alpha_f = 5^{\circ}$	α_t =c5˚	$\Lambda = 3.5$	$C = 2966$ mm

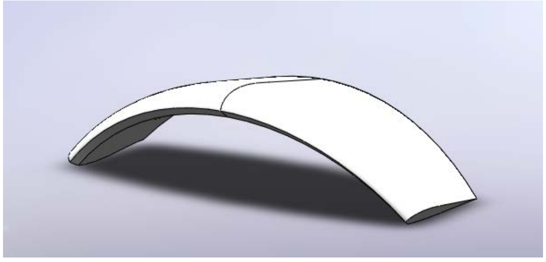

Figure 1. The model of the parafoil without bulges.

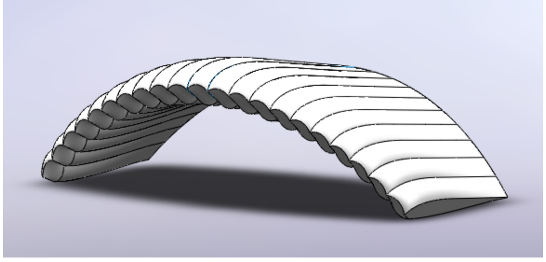

Figure 2. The model of the parafoil with bulges.

outward under the action of the inner cavity air to form a bulge in each air chamber, which will affect the aerodynamic performance of the parafoil. The degree of bulging of the parafoil is defined by "bulging relaxation *R*":

$$R = \frac{s - e}{e} \tag{1}$$

where, *s*—the width of the fabric on the upper surface of a single air chamber; *e*—the width of the both sides of fin. In this paper, the bulging relaxation of parafoil is determined to be 10% according to experience [8], the model of the parafoil with bulges is shown by **Figure 2**.

3. Numerical Simulation

The aerodynamic performance of the designed parafoil is investigated by means of CFD numerical simulation, and the bulge and leading edge air inlet of the parafoil are also investigated [9].

3.1. The Grids of Computational Domain

That the grids of parafoil flow field's computational domain are used for numerical simulation is mixed grids of structured mesh and boundary layer tetrahedral unstructured mesh. The boundary layer mesh is added near the parafoil wall, Y^+ is in the range of 1 - 5, the total number of grid cells is about 2.8 million. The distance between the outer boundary of the computational domain and the parafoil is more than 10 body lengths, and the density of the mesh is reduced in the far field to reduce the calculation amount. In the area near the wall, the mesh refinement processing method is adopted to ensure the calculation conditions of the boundary layer, and the mesh encryption is performed on the tip parts such as the tail end of the parafoil to ensure the accuracy. The grids around the parafoil are shown in **Figure 3**, and the local encrypted grids are shown in **Figure 4**.

3.2. Computational Condition

Since the main material of the parafoil is flexible fabric, the shape of the parafoil is uncertain and complicated in the actual gliding process, the following assumptions are made for the model in the simulation:

1) The parafoil is regarded as a rigid model during gliding, and the canopy does not deform during gliding;

2) Assuming that the air permeability of the canopy fabric is 0, the influence of surface air permeability on aerodynamic performance is ignored;

3) The aerodynamic performance of the main body of the parafoil is studied without considering the aerodynamic effects of the rope and the hanging ribs.

The above assumptions can shorten the computational cost of the parafoil, shorten the simulation time, and ensure the accuracy of the simulation. However, in real cases, the air permeability of the parafoil material will reduce the rigidity of the parafoil, and the air flow through the fabric of the parafoil will

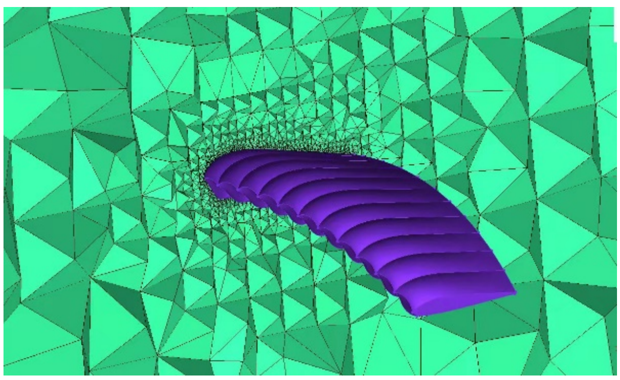

Figure 3. The grids around the parafoil.

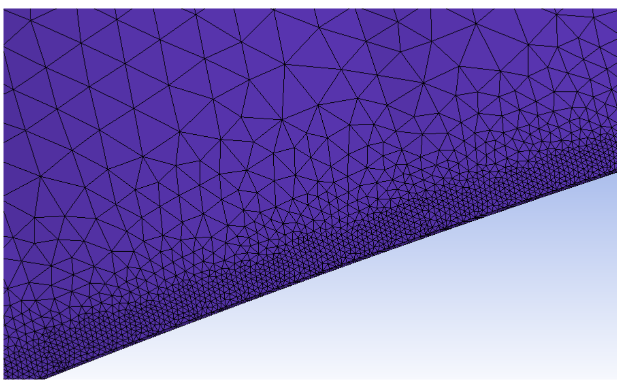

Figure 4. The local encrypted grids.

destroy the boundary layer, resulting in its separation, which will affect the lift resistance characteristics of the parafoil.

In order to investigate the effect of open leading edge and closed leading edge on numerical simulation results and the effect of open leading edge on aerodynamic performance of ramjet parafoil in CFD calculation. For the parafoil model without bulges, the leading edge is set as a closed state during simulation. For the parafoil model with bulges, the calculation is divided into two states: the open leading edge and closed leading edge. The calculation conditions of study object 1 and study object 2 are shown in **Table 2**.

Since the parafoil is a low-speed aircraft, the air around the parafoil can be regarded as incompressible flow. Finite volume method is adopted to solve the incompressible Reynolds time mean Navier-Stokes equation, and k-ω (SST) two-equation model is adopted for turbulence model. The model has a good simulation effect for outflow with inverse pressure gradient and separation. The solution algorithm is SIMPLE.

3.3. Numerical Simulation Results Analysis

3.3.1. Aerodynamic Characteristics of the Parafoil

The lift coefficient, drag coefficient and lift-drag ratio of each calculation model change with the angle of attack at -2˚, 0˚, 2˚, 4˚, 6˚, 8˚, 10˚, 12˚, 14˚, 16˚, 18˚ and 20˚, which are shown in **Figures 5-7**.

Table 2. The calculation conditions.

Angle of attack	Angular interval	Flight speed	Sea level altitude
0˚ - 20˚	$\Delta\alpha = 2˚$	12 m/s	$H = 0$ km

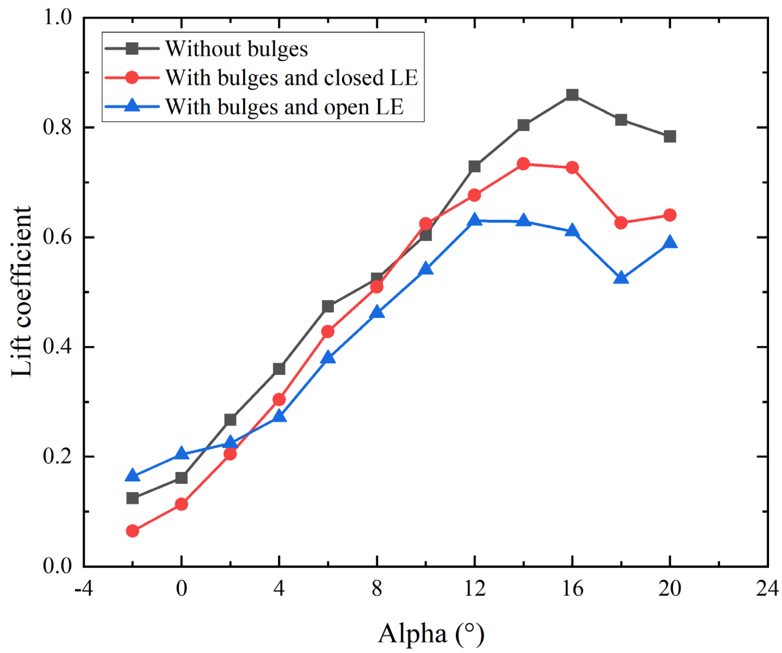

Figure 5. The lift coefficient of each calculation model.

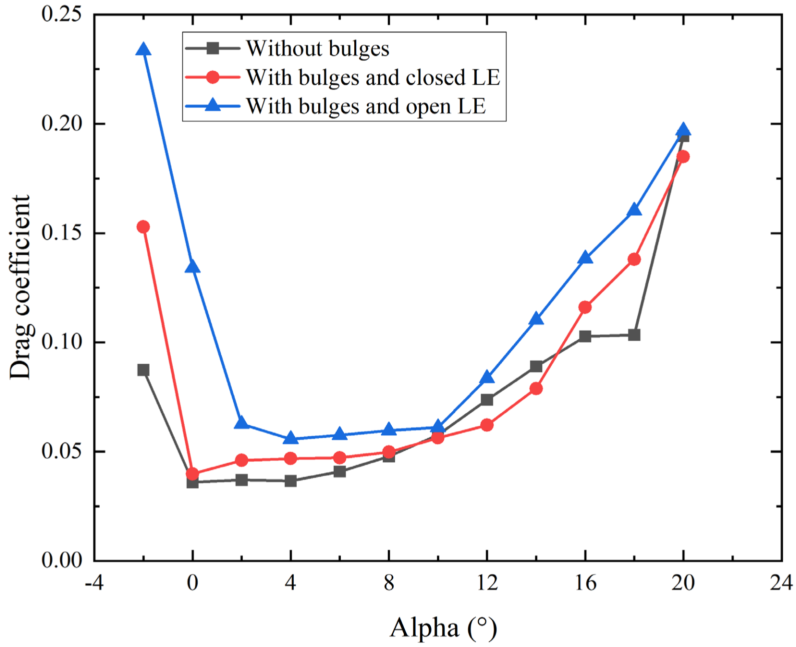

Figure 6. The drag coefficient of each calculation model.

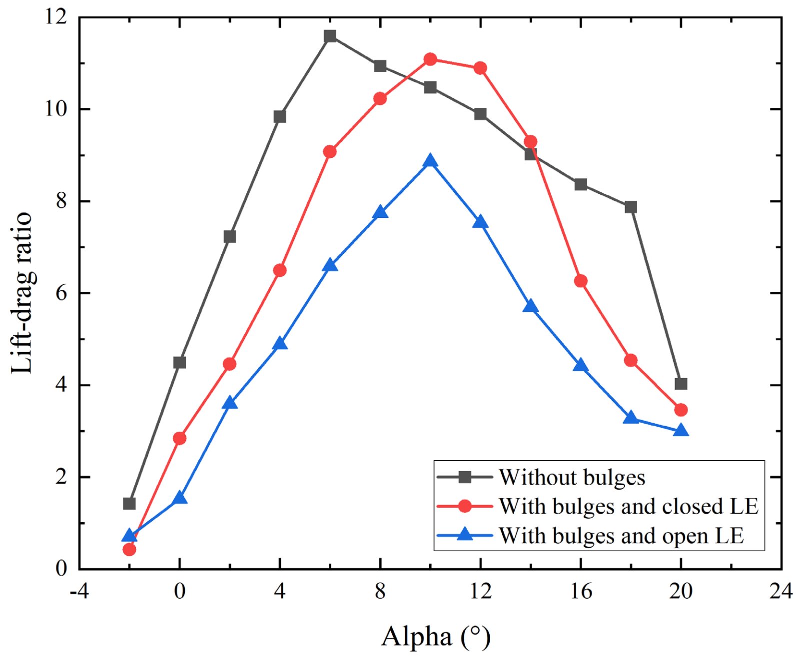

Figure 7. The lift-drag ratio of each calculation model.

The following conclusions can be drawn from the calculation results:

1) The aerodynamic parameters of the parafoil designed in this paper conform to the general rule. With the increase of the angle of attack, the lift coefficient of the parafoil increases rapidly, while the drag coefficient increases slowly. When the angle of attack increases to the optimal angle, the drag coefficient begins to increase at a faster speed. The lift-drag ratio increases with the increase of the angle of attack. When the angle of attack increases to the optimum angle of at-

tack, the lift-drag ratio begins to decrease with the increase of angle of attack.

2) The optimal angle is about 6˚, and the corresponding maximum lift-drag ratio is about 11.59. The optimum angle of attack of the bulge model is about 10˚, in which the maximum lift-drag ratio of the closed leading edge model is about 11.09, and that of the open leading edge model is about 8.86. Both the bulge and the open leading edge will reduce the aerodynamic performance of the parafoil, in which the bulge has little effect on the performance of the parafoil, and the ram intake has a greater effect on the aerodynamic performance of the parafoil.

3) The stalling angle of attack of the parafoil is 16˚ without the bulge, about 14˚ for the model with the closed leading edge and about 12˚ for the model with the open leading edge. Therefore, the bulge will cause the parafoil to stall in advance, and the open leading edge will also reduce the stalling angle of attack, affect the aerodynamic performance of the parafoil.

3.3.2. Pressure Distribution and Flow Field of Parafoil

In this paper, for the design of the non bulge model and the bulge model with leading edge and open leading edge, the chordwise pressure cloud image, the upper and lower airfoil pressure cloud image and the chordwise flow field image of the parafoil at the angle of attack of 0˚, 8˚, 12˚, and 20˚ are generated, and the distribution of the parafoil pressure and flow field at different alphas are studied, as shown in **Figures 8-11**.

As can be seen from the pressure distribution images, with the increase of the angle of attack, the lower airfoil pressure of the parafoil gradually increases, while the top airfoil pressure gradually decreases. At the same time, the leading edge of the top airfoil gradually appears negative pressure area, which spreads from the middle to both sides. Due to the influence of the open leading edge of

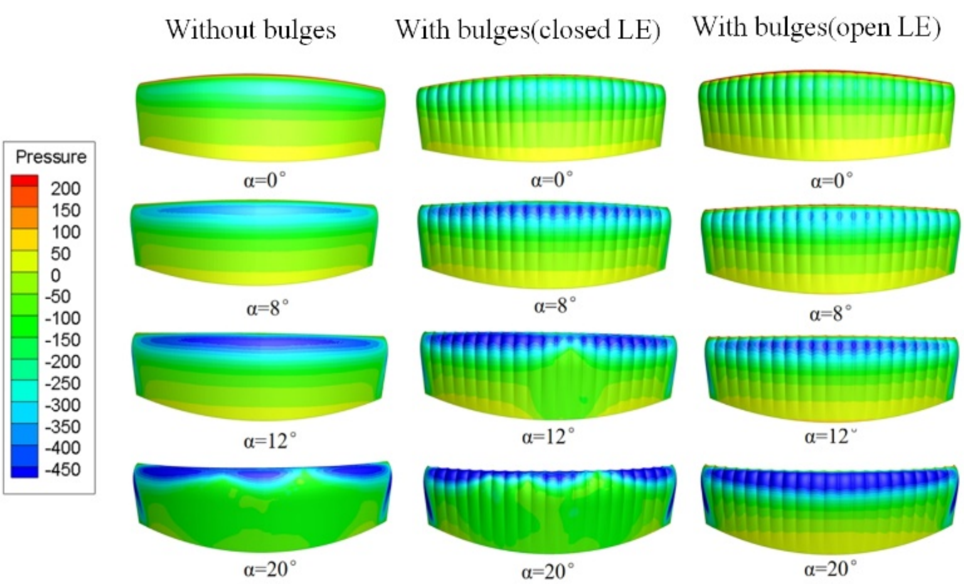

Figure 8. Pressure distribution of top parafoil.

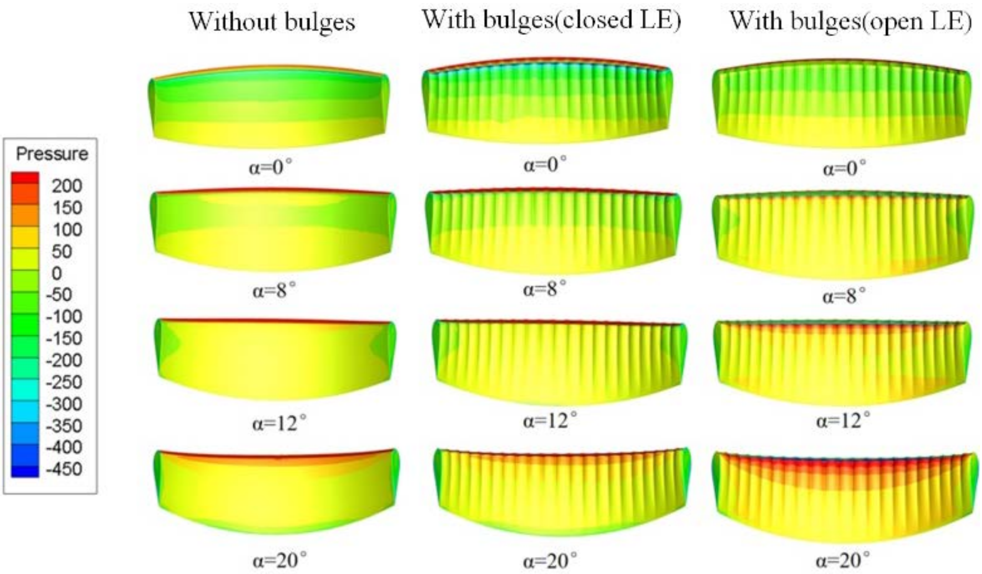

Figure 9. Pressure distribution of lower parafoil.

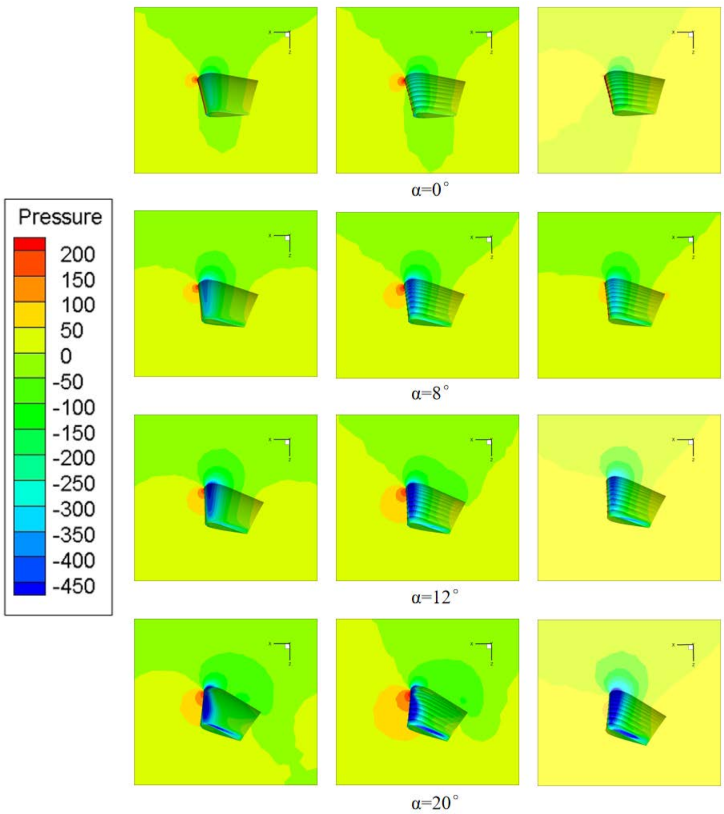

Figure 10. The chordwise pressure cloud image.

the parafoil, part of the air flow enters the inner cavity of the parafoil, which reduces the airflow around the parafoil and reduces the airflow speed. Therefore, the pressure of the top and lower airfoil of the ramjet parafoil with the open leading edge is greater than that of the ramjet parafoil with the closed leading edge.

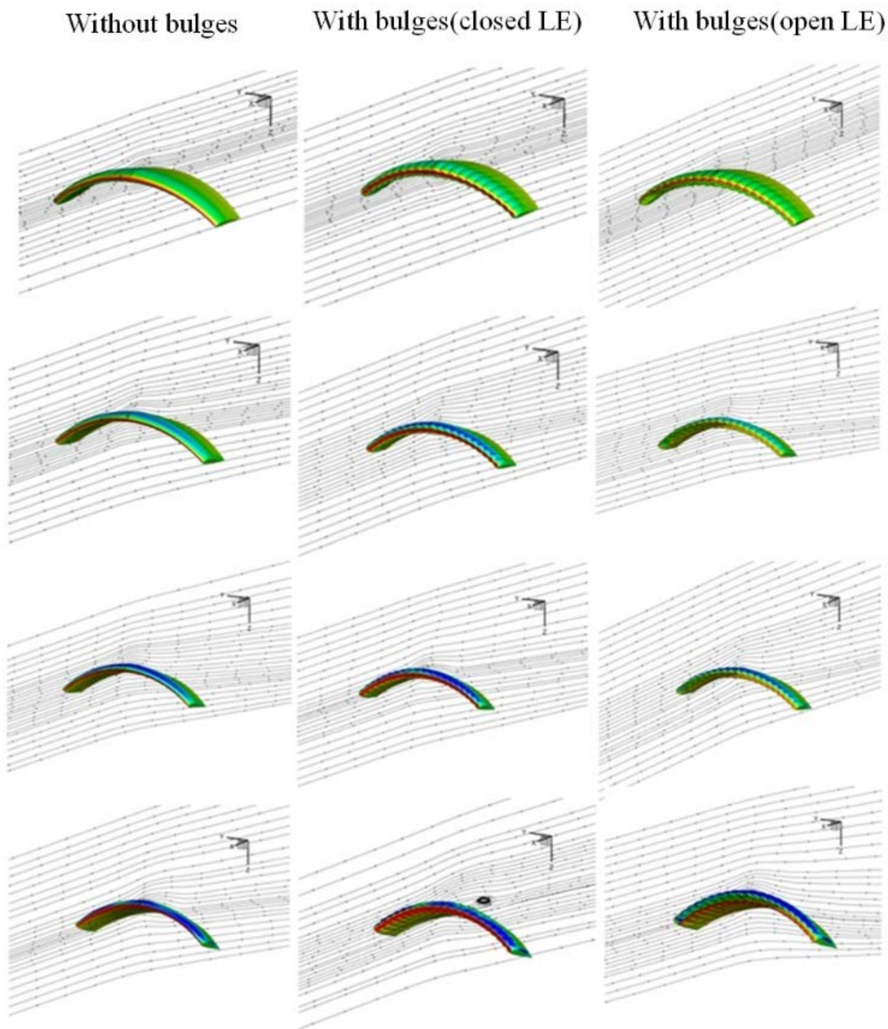

Figure 11. Chordwise fluid streamlines.

As can be seen from the chordwise pressure cloud image, due to the impact of air flow on the closed wall of the open leading edge, a high pressure region will be generated at the leading edge with the closed leading edge of the parafoil, and the distribution area of the high pressure region will gradually increase with the increase of the angle of attack, while the wide range of high pressure region will not appear in the parafoil with open leading edge. With the increase of the angle of attack, the negative pressure area of the top airfoil gradually increases, while the positive pressure area of the lower airfoil also gradually increases, which indicates that the lift-drag increases with the increase of angle of attack. When the angle of attack increases to 20˚, the positive pressure area of the lower airfoil decreases, which indicates that the parafoil has stalled at this angle of attack.

It can be seen from the chordwise fluid streamlines that there is no obvious flow separation at the optimum angle of attack, and the fluid streamlines' distribution is uniform, which is in line with the design requirements of the parafoil. However, in the bulge model with closed leading edge, an obvious vortex is generated on top airfoil at 20˚. The reason is that the bulge increases the thickness of the airfoil, and the angle of attack is too large, which intensifies the airflow separation. At the same time, the pressure on the top airfoil is lower than that of the open leading edge, which results in a vortex.

4. Conclusion

In summary, we conducted CFD numerical simulation on three different configurations of the ram-air parafoil with bulges and open/closed ram-air inlet to study the aerodynamic characteristics and flow mechanism of the ram-parafoil. The results of the study show that compared with the aerodynamic parameters of the parafoil without bulges, the optimal angle of attack of the two parafoils with bulges is increased by 4˚, the maximum lift to drag ratio of the parafoil with closed leading edge is reduced by about 4.3% and the stall angle of attack is reduced by about 2˚. The maximum lift to drag ratio of the parafoil with open leading edge is reduced by about 23.6% and the stall angle of attack is reduced by about 4˚. The pressure on the surface of a ram-air parafoil with open leading edge inlet is the highest.

Conflicts of Interest

The authors declare no conflicts of interest regarding the publication of this paper.

References

[1] Matos, C., Mahalingam, R., Ottinger, G., Klapper, J. and Funk, R. (1998) Wind Tunnel Measurements of Parafoil Geometry and Aerodynamics. 36*th AIAA Aerospace Sciences Meeting and Exhibit*, Reno, 12-15 January 1998, AIAA Paper 98-0606. https://doi.org/10.2514/6.1998-606

[2] Seidel, J., Latscha, C., Venkataraman, G., Bergeron, K. and McLaughlin, T.E. (2016) Rigid Ram-Air Parachute Experiments with Bleed Air Vents. 54*th AIAA Aerospace Sciences Meeting*, San Diego, 4-8 January 2016, AIAA 2016-1562. https://doi.org/10.2514/6.2016-1562

[3] Bergeron, K., Seidel, J. and McLaughlin, T.E. (2015) Wind Tunnel Investigations of Rigid Ram-Air Parachute Canopy Configurations. 23*rd AIAA Aerodynamic Decelerator Systems Technology Conference*, Daytona Beach, 30 March-2 April 2015, AIAA 2015-2156. https://doi.org/10.2514/6.2015-2156

[4] Machin, R.A., Iacomini, C.S., Cerimele, C.J. and Stein, J.M. (2001) Flight Testing the Parachute System for the Space Station Crew Return Vehicle. *Journal of Aircraft*, **38**, 786-799. https://doi.org/10.2514/2.2854

[5] Iacomini, C. and Madsen, C. (1999) Investigation of Large Scale Parafoil Rigging Angles-Analytical and Drop Test Results. 15*th Aerodynamic Decelerator Systems Technology Conference*, Toulouse, 8-11 June 1999, 1752-1753. https://doi.org/10.2514/6.1999-1752

[6] Balaji, R., Mittal, S. and Rai, A.K. (2005) Effect of Leading Edge Cut on the Aerodynamics of Ram-Air Parachutes. *International Journal for Numerical Methods in Fluids*, **47**, 1-17. https://doi.org/10.1002/fld.779

[7] Dunker, S. (2013) Ram-Air Wing Design Considerations for Airborne Wind Energy. *Airborne Wind Energy*. Springer Berlin Heidelberg, Berlin, Heidelberg, 517-546.

https://doi.org/10.1007/978-3-642-39965-7_31

[8] Fogell, N.A., Iannucci, L. and Bergeron, K. (2017) Fluid-Structure Interaction Simulation Study of a Semi-Rigid Ram-Air Parachute Model. 24*th AIAA Aerodynamic Decelerator Systems Technology Conference*, Denver, 5-9 June 2017, 3547-3548. https://doi.org/10.2514/6.2017-3547

[9] Ghoreyshi, M., Bergeron, K., Seidel, J., Jirásek, A. and Lofthouse, A.J. (2016) Prediction of Aerodynamic Characteristics of Ram-Air Parachutes. *Journal of Aircraft*, **53**, 1802-1820. https://doi.org/10.2514/1.C033763